1990

Finite temperature structure and thermodynamics of the Au Σ5 (001) twist boundary

R. Najafabadi
D. J. Srolovitz
Richard Alan Lesar, *Los Alamos National Laboratory*

Finite temperature structure and thermodynamics of the Au Σ5 (001) twist boundary

R. Najafabadi and D. J. Srolovitz
Department of Materials Science and Engineering, University of Michigan, Ann Arbor, Michigan 48109

R. LeSar
Theoretical Division, Los Alamos National Laboratory, Los Alamos, New Mexico 87545

(Received 20 December 1989; accepted 26 July 1990)

The structure and thermodynamic properties of a Σ5 (001) twist boundary in gold are studied as a function of temperature. This study was performed within the framework of the Local Harmonic (LH) model and employed an Embedded Atom Method (EAM) potential for gold. We find that for the Σ5 (001) twist boundary in gold, a distorted CSL structure is stable at low temperatures, but undergoes a phase transformation to a DSC related structure near room temperature. This transformation is shown to be first order. The temperature dependences of the excess grain boundary free energy, enthalpy, entropy, specific heat, and excess volume are calculated. Discontinuities are observed in the slope of the grain boundary excess free energy (versus temperature), in the value of the grain boundary excess specific heat and excess volume. The stable high temperature grain boundary structure has a smaller excess volume than does the lower temperature structure, and both structures have a coefficient of thermal expansion which is in excess of that for the perfect crystal.

I. INTRODUCTION

The atomistic structure of grain boundaries has been the subject of active investigation over the past two decades. In general, there has been good agreement between experimentally determined grain boundary structures and those obtained through atomistic computer simulations. One particular grain boundary in gold has received more attention than any other grain boundary. This grain boundary is the Σ5 (001) twist boundary, which corresponds to a relative rotation (36.9°) of two crystals along their common [001] axis such that one out of five of the atoms would be in coincidence if the two crystals were interpenetrating. The reason for this attention may be attributed to the fact that this boundary is one of the simplest high-angle grain boundaries, and yet general agreement between experiment and simulation has not yet been achieved.[1–3] This disagreement may be due to the fact that the simulations and experiments were performed at different temperatures and the existence of different possible grain boundary structures with very similar energies. The purpose of the present paper is to determine the *finite temperature* structure and thermodynamic properties of the Σ5 (001) twist boundary in gold. We find that this grain boundary undergoes a first order phase transition at a temperature very close to room temperature.

X-ray diffraction techniques have been used extensively, in recent years, to analyze the structure of twist grain boundaries in gold.[1–5] The measured integrated intensities of the diffraction points due to the grain boundary are used to determine the atomic structure that provides the best fit with experiment[2–4] or to test the validity of a proposed structure which has been predicted on the basis of atomistic computer simulations.[3] In the case of the Σ5 (001) (36.9°) twist boundary in gold, there has been some disagreement between the atomic structures constructed based on x-ray diffraction observations[1,2] and the atomic structure predicted by atomistic computer simulations. A recent x-ray diffraction study[3] of the same grain boundary, however, shows good agreement with the simulated structure.

It has recently been suggested[6] that part of the discrepancy between the simulation and experimental results may be attributed to thermal effects. The experimental samples were prepared at an elevated temperature and the diffraction experiments were performed at nominal room temperature.[7] The simulations, on the other hand, were performed at $T = 0$. If the grain boundary were to exhibit a structural phase transition between $T = 0$ and room temperature (or between $T = 0$ and the sample preparation temperature), there would be no reason to expect agreement between the simulated and experimental structure. Both experimental[8] and simulation[9] evidence exists for the existence of grain boundary structural phase transitions. Guillope[9] reported molecular dynamics evidence for a structural phase transition in a tilt boundary using a Lennard–Jones potential. Vitek *et al.*[10] showed simulation/theoretical evidence for a grain boundary struc-

tural disordering transition. Experimentally, grain boundary faceting transitions have been observed.[8] In addition, there has been considerable debate as to whether premelting occurs at grain boundaries (for a review, see Ref. 8). Largely in conjunction with the atomistic studies of grain boundary melting, simulation results on the thermodynamic properties of a restricted set of grain boundaries have become available.[11–16] The observations and theory relating to phase transitions at internal interfaces have recently been reviewed by Rottman.[17]

In the present paper, we present simulation results on the temperature dependence of the structural and thermodynamic properties of the Σ5 (001) (36.9°) twist grain boundary in gold. We find that a first order structural transition occurs very near room temperature. These calculations were performed by minimizing the *free energy* of a bicrystal with respect to the atomic coordinates and the relative positions of the two crystals. The approximate free energy of the atomic system containing the grain boundary was determined within the framework of the recently introduced local-harmonic (LH) model[18] (which is a variant of the Einstein model) with the atomic interactions described in terms of the embedded atom method (EAM) potential for gold.[19] Using the LH model, we have examined the stability of many of the different atomic structures proposed for the $\Sigma = 5$ (001) twist boundary over a temperature range of $0 \leqslant T\,(\mathrm{K}) \leqslant 700$.

In the local harmonic (LH) model,[18] the true vibrational density of states, $N(\omega)$, is replaced by a summation over the local density of states (LDOS), $n_i(\omega)$, which is described as a sum of delta functions centered at the three distinct local vibrational frequencies for each atom. These local frequencies may be determined by diagonalizing the local dynamical matrix. This assumption is equivalent to a local Einstein model. The LH model was preceded by a similar model proposed by Sutton.[14] In Sutton's model, the LDOS is determined by calculating the second moment of the local density of states from the trace of the local dynamical matrix. Since the trace of a matrix is invariant with respect to rotation, the second moment then depends on the sum of the square of the three fundamental vibrational frequencies. Sutton then assumes a functional form for the density of states that has the correct square-root singularities at the band edges. This approximate density of states $N(\omega)$ is then used in Eq. (1) to determine the free energy. The essential difference between the LH model and that developed by Sutton is in the approximation to the LDOS. Since Sutton's assumed form of the LDOS better approximates the shape of the true LDOS for a single band, we expect that Sutton's model will be more accurate for perfect crystals than the LH model (including yielding the proper T^3 specific heat temperature dependence at very low T). However, since in the LH model the width and mean of the LDOS are independent, we expect that the LH model will be more appropriate for defect studies where the local atomic environments are anisotropic and will likely result in a broader LDOS than would be expected in the perfect crystal for the same mean vibrational frequency. The LH model may be easily extended, along the lines suggested by Sutton, by replacing each of the three vibrational frequencies with an appropriate frequency distribution.

The details of the local harmonic model for the free energy of the system will be discussed in the next section along with its application to a perfect crystal. Section III describes the simulation method employed in the present study of the Σ5 (001) (36.9°) twist grain boundary in gold. The determination of the equilibrium atomistic structure of this grain boundary is then determined as a function of temperature and the scattering factors are determined. Section V reports the thermodynamic properties of this boundary.

II. LOCAL HARMONIC MODEL

The quasiharmonic approximation to the free energy of a solid[20] has been shown to be very accurate up to temperatures in the vicinity of the melting point. Within the framework of this model, the Helmholtz free energy may be written as

$$A_0 = U + \mathrm{k_B}T \int_0^\infty N(\omega) \ln\left[2\sinh\left(\frac{\mathrm{h}\omega}{4\pi \mathrm{k_B}T}\right)\right] d\omega \tag{1}$$

where U is the total potential energy, h is Planck's constant, ω is the vibrational frequency, $\mathrm{k_B}T$ is the thermal energy, and $N(\omega)$ is the vibrational density of states.

In the recently developed local harmonic (LH)[18] variant of the Einstein model, one neglects all terms that couple vibrations of different atoms in the quasiharmonic approximation. This approximation essentially decomposes the full $3N \times 3N$ dynamical matrix into N 3×3 local dynamical matrices, where N is the number of atoms in the system. Diagonalization of these matrices provides $3N$ local vibrational frequencies, $\omega_{\beta i} (\beta = 1, 2, 3)$, which are then used in Eq. (1). The integral over the full vibrational density of states $N(\omega)$ in Eq. (1) is thus replaced by a sum over these $3N$ vibrational frequencies. In this (LH) approximation, the free energy may be written as

$$A_0 = U + \mathrm{k_B}T \sum_{i=1}^{N} \sum_{\beta=1}^{3} \ln\left[2\sinh\left(\frac{\mathrm{h}\omega_{\beta i}}{4\pi \mathrm{k_B}T}\right)\right] \tag{2}$$

where the sum on i is over all atoms and the sum on β is over the 3 vibrational frequencies of atom i. The LH model has previously been employed to calculate the free energy of a perfect crystal and the formation free

energy of a vacancy as a function of temperature in copper, as described by a Morse potential. The results obtained with the LH model were shown to be in excellent agreement with the thermodynamic properties (including free energy) determined via a series of Monte Carlo simulations.[18]

In the present study, the atomic interactions are described by the embedded atom method (EAM) potential for gold.[19] Within the framework of the EAM, the total potential energy of the system is given by

$$U = \frac{1}{2}\sum_{i=1}^{N}\sum_{j\neq i}\varphi(r_{ij}^{0}) + \sum_{i=1}^{N}F_i\left(\sum_{j\neq i}\rho(r_{ij})\right) \tag{3}$$

where φ_{ij} is the pair interaction between atoms i and j, the sum on j is over all neighbors of i (out to some predetermined cutoff), $\rho(r_{ij})$ is the spherically averaged electron density of atom i at the position of atom j, and F_i is the energy required to embed atom i into the electron density due to all of its neighbors.

The vibrational frequencies $\omega_{\beta i}$ are given by the square root of the eigenvalues of the (3 × 3) local dynamical matrix D_i where its elements are defined by

$$D_i^{\alpha\beta} = \frac{\partial^2 U}{\partial r_i^{\alpha}\partial r_i^{\beta}} \tag{4}$$

and where α and β indicate directions. In the classical limit ($h\omega \ll k_B T$), Eq. (2) can be simplified to

$$A_0 = U + 3k_B T\sum_{i=1}^{N}\ln\left[\frac{|D_i|^{1/6}}{2\pi k_B T m^{1/2}}\right] \tag{5}$$

where $|D_i| = m^3[\omega_{1i}\omega_{2i}\omega_{3i}]^2$ is the determinant of the local dynamical matrix of atom i, and $|D_i|^{1/6}$ is the geometric average of the vibrational frequencies of atom i. The finite temperature pseudoforce (i.e., the thermally averaged force) on atom i in the β direction is

$$f_{i\beta} = -\frac{\partial A_0}{\partial r_{i\beta}} = -\frac{\partial U}{\partial r_{i\beta}} + \frac{1}{2}k_B T\sum_{j=1}^{N}\frac{1}{|D_j|}\frac{\partial |D_j|}{\partial r_{i\beta}} \tag{6}$$

The equilibrium atomic structure and corresponding thermodynamic properties are determined by minimizing the total free energy of the system (at any temperature) with respect to the atomic coordinates. For a perfect crystal (such as fcc gold), the free energy minimization is reduced to a minimization with respect to one variable, the lattice constant a_0. The lattice constant, Gibbs free energy, enthalpy, and entropy of a perfect fcc gold crystal described by the LH model and the EAM Au potential were determined as a function of temperature for zero pressure. These data are plotted in Fig. 1 together with the available experimental data.[21] The agreement between the simulation predictions and experiment for the studied temperature range (0 to 1000 K) is excellent. The free energy data in Fig. 1(b) are also compared with data from a recent Monte Carlo computer simulation by Foiles[20] using the same potential. As with our previous work[18] using a Morse potential, the LH slightly overestimates the free energy of the solid (described by the same potential). The overall excellent agreement among the Monte Carlo, experimental, and LH data suggests that the LH model is a good approximation to the true free energy and that the EAM potential is a reasonable representation of the Au atomic interactions.

The excess thermodynamic properties associated with defects in the system may be calculated as

$$\Delta\Psi = \Psi_{\text{system}} - \Psi_{\text{perfect}} \tag{7}$$

where Ψ_{system} and Ψ_{perfect} are the values of the thermodynamic property of the atomic system with the defect and assuming that all of the atoms are in a perfect crystal at the proper temperature-dependent lattice parameter, respectively. $\Delta\Psi_{gb}$ is the corresponding excess grain boundary property, where Ψ could refer to the free energy, entropy, enthalpy, volume, etc. It is convenient to normalize $\Delta\Psi_{gb}$ by the area of the grain boundary, and hence the quoted excess thermodynamic properties are all so normalized.

Since atomic structural data are often interpreted on the basis of scattering experiments, we analyze the finite temperature scattering intensity. The scattering intensity, $I_{hkl} = \langle|F_{hkl}(T)|^2\rangle$, can be written as

$$I_{hkl} = \langle|F_{hkl}(T)|^2\rangle = \left|\sum_{i=1}^{N}\exp[-2\pi^2\langle r_i^2\rangle K/d_{hkl}^2]\exp[2\pi i\mathbf{R}_i\mathbf{K}]\right|^2 \tag{8}$$

where d_{hkl} is the spacing between adjacent hkl planes and $\langle r_i^2\rangle K$ is the mean square displacement of atom i along the $\mathbf{K}$ direction. In the LH model, the mean-square displacement can be expressed by[21]

$$\langle r_i^2\rangle_K = \frac{k_B T}{m}[(K_x/\omega_{xi})^2 + (K_y/\omega_{yi})^2 + (K_z/\omega_{zi})^2]d_{hkl}^2 \tag{9}$$

where $\omega_{xi}, \omega_{yi}, \omega_{zi}$ are calculated from the dynamical matrix tensor [Eq. (4)] and K_x, K_y, and K_z are components of vector $\mathbf{K}$ in the normal mode coordinates of atom i. Since the atomic environments vary from atom to atom in the vicinity of a grain boundary, it is important to replace the classical Debye–Waller correction term[22] with one that takes into account the different local atomic vibrational frequencies. This gives rise to a $\mathbf{K}$ dependent Debye–Waller factor.

III. SIMULATION METHOD

In simulating atomic systems containing defects, such as grain boundaries, special care must be exercised in choosing appropriate boundary conditions. The inhomogeneity inherent in the defect region must not be constrained by the choice of boundary conditions and it must be free to change when the external conditions

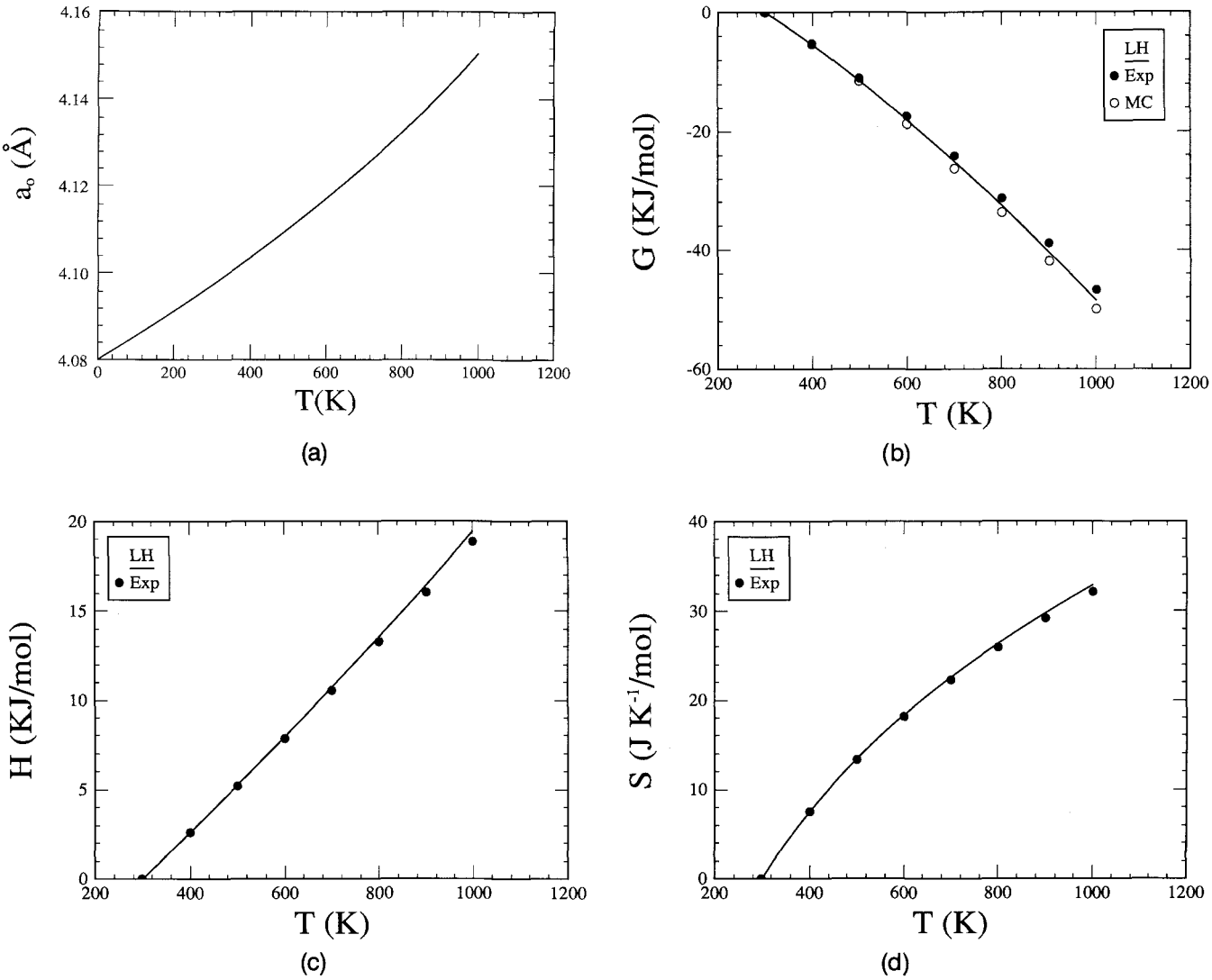

FIG. 1. The (a) lattice constant a_0, (b) Gibbs free energy G, (c) enthalpy H, and (d) entropy of a perfect crystal of gold (solid lines) determined by the LH model employing the EAM gold potential. The thermodynamic data are plotted relative to the T = 300 K data. The filled symbols in (b)–(d) correspond to experimental measurements,[16] and the open symbols in (b) are Monte Carlo determinations,[15] which employed the same EAM potential as that used here.

(e.g., temperature and/or stress) are modified. For any finite Σ value (reciprocal coincident lattice site density), grain boundary structures are periodic in the boundary plane (x-y plane, since the twist boundary rotation axis is [001]); therefore, a bicrystal with periodic boundary conditions in the x and y directions is employed. Since the present simulations are performed at zero stress (for the perfect crystal), the distance over which the simulation cell is periodic is scaled by the temperature dependent, perfect crystal lattice constant. The crystals on either side of the grain boundary are free such that relative shifts of the two crystals, parallel and perpendicular to the boundary plane, are not constrained.

A schematic of the simulation cell employed in the present simulations is shown in Fig. 2. The simulation cell is divided into two regions, I and II. The atoms in region I are completely free to move in response to forces due to the other atoms. The atoms in region II, however, are constrained such that region II is a perfect crystal with the lattice parameter appropriate for the simulation temperature. The equilibrium atomic configuration is obtained by minimizing the free energy [Eq. (5)] with respect to the coordinates of the atoms in region I and the relative positions of the upper and lower crystals. Addition of the three variables corresponding to the relative positions of the two crystals removes all constraints on the relative in-plane translation of the two crystals and on the expansion in the z-direction, which may occur if the excess volume of the grain boundary is not zero. This type of simulation geometry guarantees that a perfect crystal is at zero net

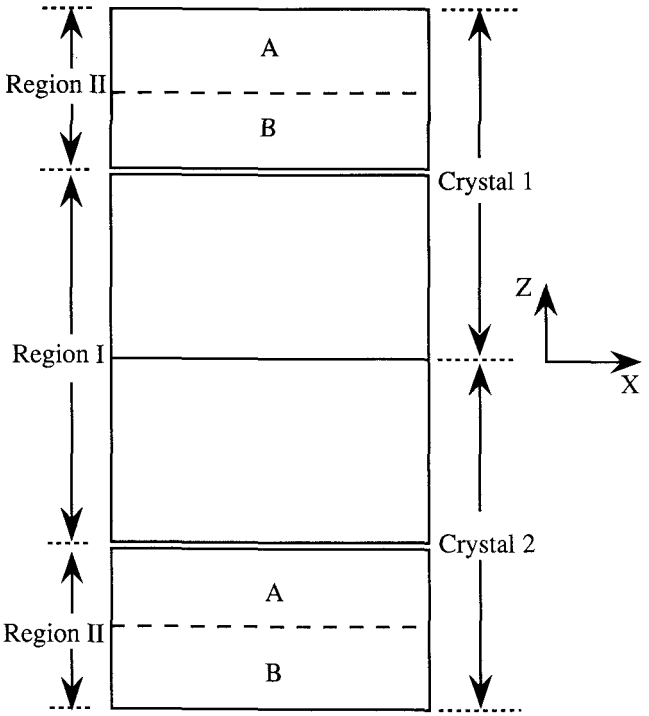

FIG. 2. The simulation cell employed in the present grain boundary simulations. The grain boundary is in the middle of region I. The atoms in region I are each free to move, while those in region II move rigidly with the rest of the crystal. Crystals I and II are free to translate with respect to each other.

stress. However, since the periodicity in the x and y directions is fixed by the perfect crystal, some net stress may develop in the grain boundary region. This is appropriate, since typical grain sizes are extremely large compared to the boundary width.

Region II is divided into two sub-regions, A and B, the extent of which is determined by the cutoff radius for the interatomic potential. Atoms in region IIB are at fixed relative positions and by virtue of their proximity to region I, make a direct contribution to the free energy. Atoms in region IIA are also at fixed relative positions and interact only with the fixed atoms in region IIB. However, due to the non-pair nature of the EAM potential, the local vibrational frequencies (or $|D_i|$) in region IIA may change as the coordinates of the atoms in region I change. These changes, in turn, affect only the second term in the free energy expression [Eq. (5)].

The free energy minimization needed to find the temperature dependent, equilibrium atomic configurations is performed using a conjugate gradient relaxation method in $3N$ variables, where N is the number of atoms in region I ($3N - 3$ atomic coordinates and 3 relative crystal coordinates). The relaxation process is considered converged when the maximum "pseudo-force" $(-\partial A/\partial x_i)$ on any atom in region I is less than 10^{-5} eV/Å.

The exact extent of region I in the z direction is not determined *a priori*. Although the majority of the atomic relaxation is limited to a few atomic layers above and below the grain boundary plane, an accurate determination of the grain boundary energy requires inclusion of the elastic strain field of the grain boundary. In order to determine the number of atoms needed to obtain converged properties, a series of grain boundary [Σ5 (001)] structures were obtained by free energy minimization for different numbers of atomic layers parallel to the grain boundary. The grain boundary free energy γ_{gb} [see Eq. (7)] and the [330] [see Eq. (8)] scattering intensity were calculated as a function of the size of region I at zero temperature. Figure 3(a) shows that the energy of the Σ5 twist grain boundary is converged with respect to the size of region I with between eight and twelve atomic layers. We expect similar convergence in the other thermodynamic properties. However, Fig. 3(b) shows that for more structurally sensitive properties such as the scattering intensity, the calculations must be carried out in a cell of approximately twice that size. The simulations presented here were all performed with 18 free atomic layers parallel to the grain boundary plane.

IV. Σ5 (001) TWIST BOUNDARY STRUCTURES

Several suggestions have been made for the atomic structure of the Σ5 (001) twist boundary in metals, in general, and for that boundary in gold, in particular. The unrelaxed Σ5 (001) Coincidence Site Lattice (CSL) twist boundary structure is shown in Fig. 4, where the circles represent atomic positions in the layers closest to the boundary plane and the squares represent atomic positions in the next layers farther from the boundary. Open symbols correspond to atoms from the upper crystal, and filled symbols correspond to atoms from the lower crystal. This structure has been the primary focus of most previous simulation studies of this boundary. It has a fourfold symmetry axis parallel to (001) and both twofold and twofold-screw axes lying in the geometrical interface plane. The experimentally observed Σ5 twist boundary structure in gold is consistent with these symmetry elements.[1] Previous simulations[23] of the Σ5 (001) twist boundary have shown that the CSL structure is not always the lowest energy structure at zero temperature, depending on the choice of interatomic potentials.

Bristowe and Crocker,[23] in their search for other possible structures for this twist boundary, found two other Σ5 structures which they referred to as type I and II. The unrelaxed type I and II structures (Figs. 5 and 6) are related to the unrelaxed CSL structure by a translation vector of $(1/2)\mathbf{b}_1$ and $(1/2)(\mathbf{b}_1 + \mathbf{b}_2)$ in the grain boundary plane, respectively, where $\mathbf{b}_1 = (1/10)$ [130] and $\mathbf{b}_2 = (1/10)$ [$3\bar{1}0$] are vectors defining the

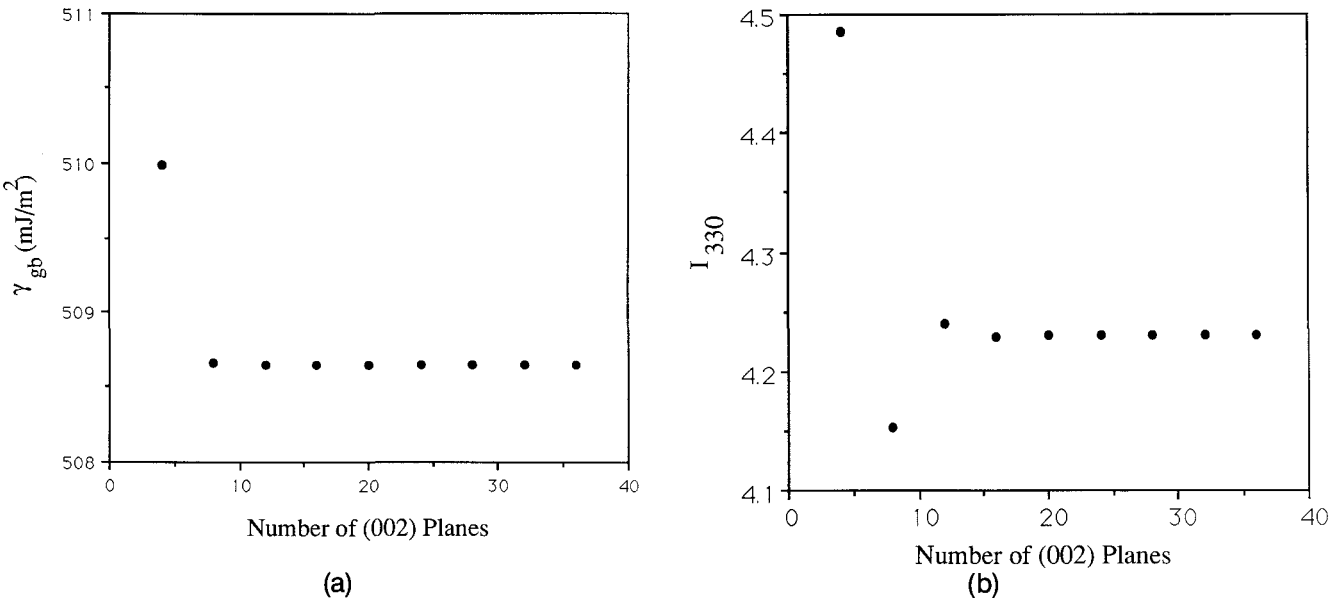

FIG. 3. Sensitivity of (a) the grain boundary free energy γ_{gb} and (b) the scattering intensity corresponding to the [330] grain boundary reflection to variations in the size of the simulation cell normal to the grain boundary plane [i.e., the number of (002) planes].

Σ5 DSC[24] (Displacement Shift Complete) sublattice. Bristowe and Crocker's zero temperature calculation, which employed pair potentials representing copper and nickel, showed that the relaxed type I and type II structures are the most stable structures for the Σ5 (001) twist boundary in copper and nickel, respectively.

Budai *et al.*[1] have constructed two additional grain boundary structures (α and β) based upon their x-ray

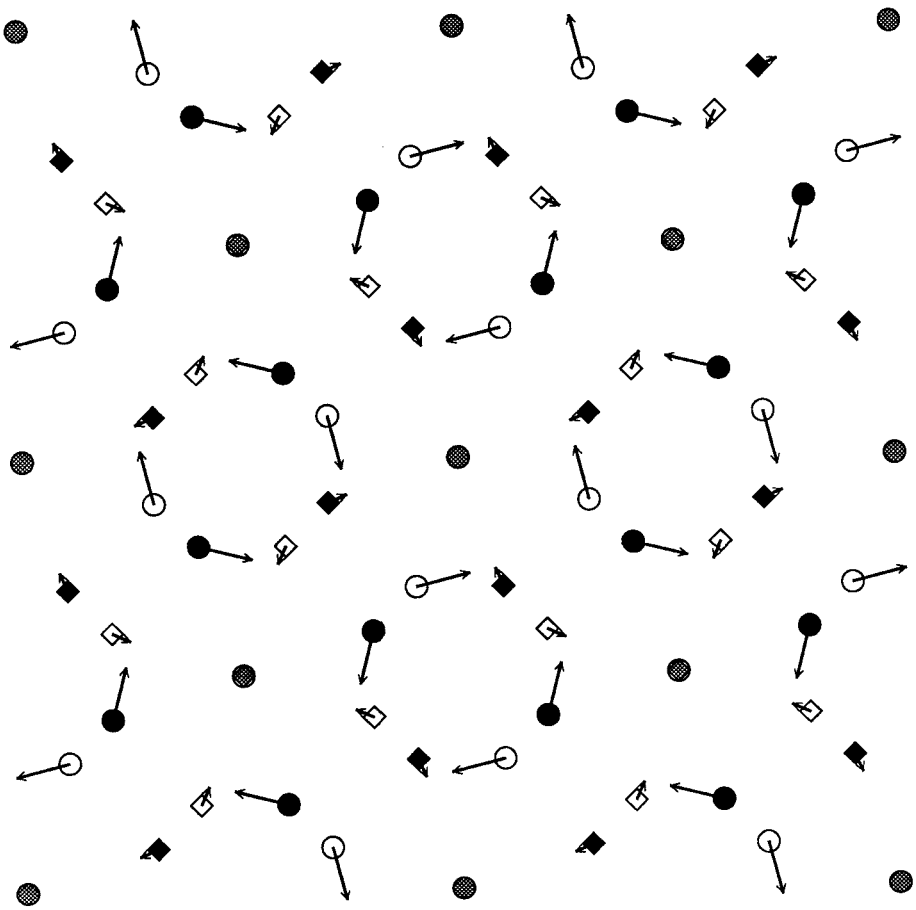

FIG. 4. The CSL structure of the Σ5 (001) twist boundary. The symbols represent the atom positions in the unrelaxed CSL structure, and the arrows indicate the displacement of the atoms upon relaxation at 300 K (the size of the arrrows has been magnified by a factor of 7.5 for clarity). The filled circles are in the nominal (002) plane immediately above the boundary plane and the filled diamonds are in the next nominal (002) plane above the boundary. The open circles represent the atomic positions in the plane immediately below the boundary, and the open diamonds are in the next plane below the boundary. The hatched symbols represent two atoms with the same (x, y) coordinates but different z-coordinates.

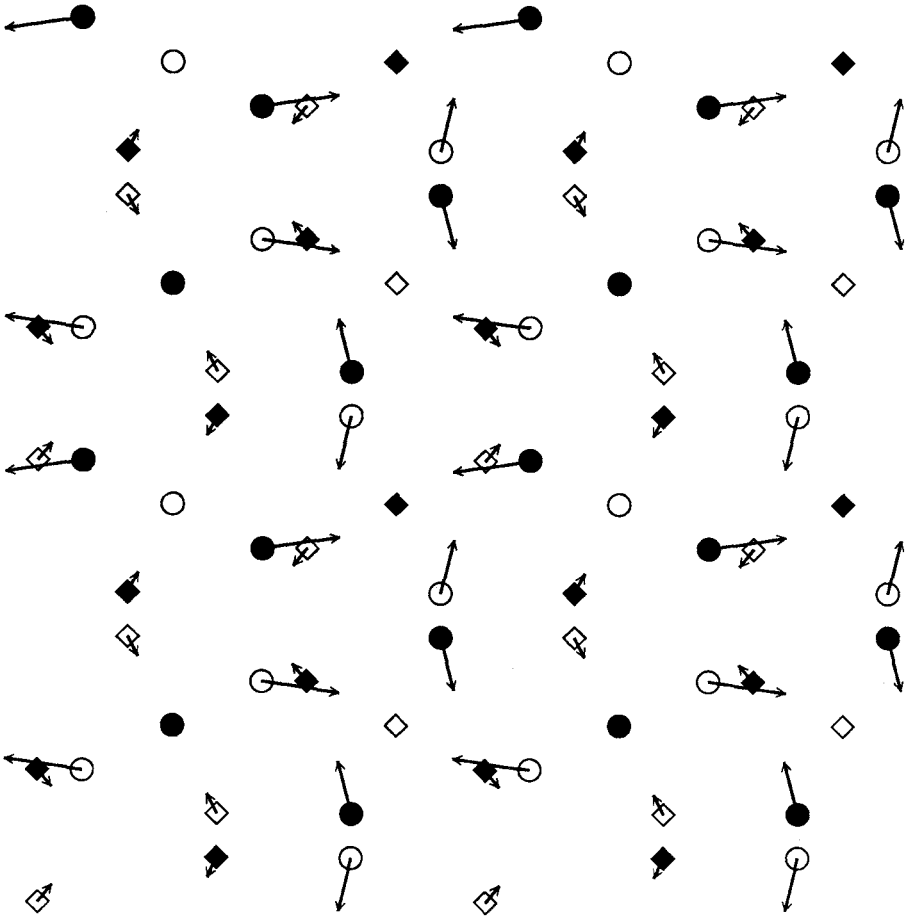

FIG. 5. The type I structure of the Σ5 (001) twist boundary. The symbols represent the atom positions in the unrelaxed type I structure, and the arrows indicate the displacement of the atoms upon relaxation at 600 K. The symbols have the same meaning as in Fig. 4.

diffraction observations. The atomic displacements away from the ideal CSL lattice for these two structures are much larger than predicted based upon atomistic simulation techniques. Recently, Fitzsimmons and Sass[2] constructed another structure α' for the Σ5 boundary from new x-ray diffraction measurements which is a variant of the α structure. This structure, like the α and β structures, possesses the symmetry of the CSL structure. All of these structures, when used as initial configurations in atomistic computer simulations, have proven to be unstable. The source of the instability is, most likely, the strong repulsive force between the atoms at the small atomic separations characteristic of these structures.[25]

Oh and Vitek[25] have proposed another structure, called A_1, which is a CSL structure with atoms in the layer just above the boundary shifted in the same way as in the α structure. This structure, Fig. 7, and its symmetry related structure, A_2, have been reported as stable structures on the basis of atomistic simulations. Assuming that these two structures coexist in the Σ5 (001) twist boundary, Oh and Vitek[25] have shown that the composite structure leads to improved agreement with the x-ray diffraction data of Budai *et al.*[1] compared to that of α and β structures.

In order to determine the most stable Σ5 (001) twist grain boundary structure at zero temperature and pressure, we constructed all of the proposed structures discussed above. For the EAM potential used in the present simulations, all of the initial structures relaxed into a variant of the ideal CSL structure, regardless of the initial atomic configurations. The relaxed structure is shown in Fig. 4 where the vectors at each atomic site represent the displacements of the atoms away from the ideal CSL structure. While the α, β, and α' structures, which were constructed solely from the experimental studies, are known to be unstable,[1,2] the A_1,[25] type I, and type II[23] structures have previously been reported to be stable at zero temperature. Although the differences in atomic potentials between the present and previous calculation may be partly responsible for these differences, one should note that all of the previous results were obtained using computer simulation methods that employ fixed overall volume.

As the temperature was increased (in 100 K increments), the simulation that started from the equilibrium $T = 0$ atomic configuration (CSL variant) remained stable. At $T = 600$ K, however, the CSL structure transformed during the course of the simulation to a relaxed form of the type I structure. This relaxed struc-

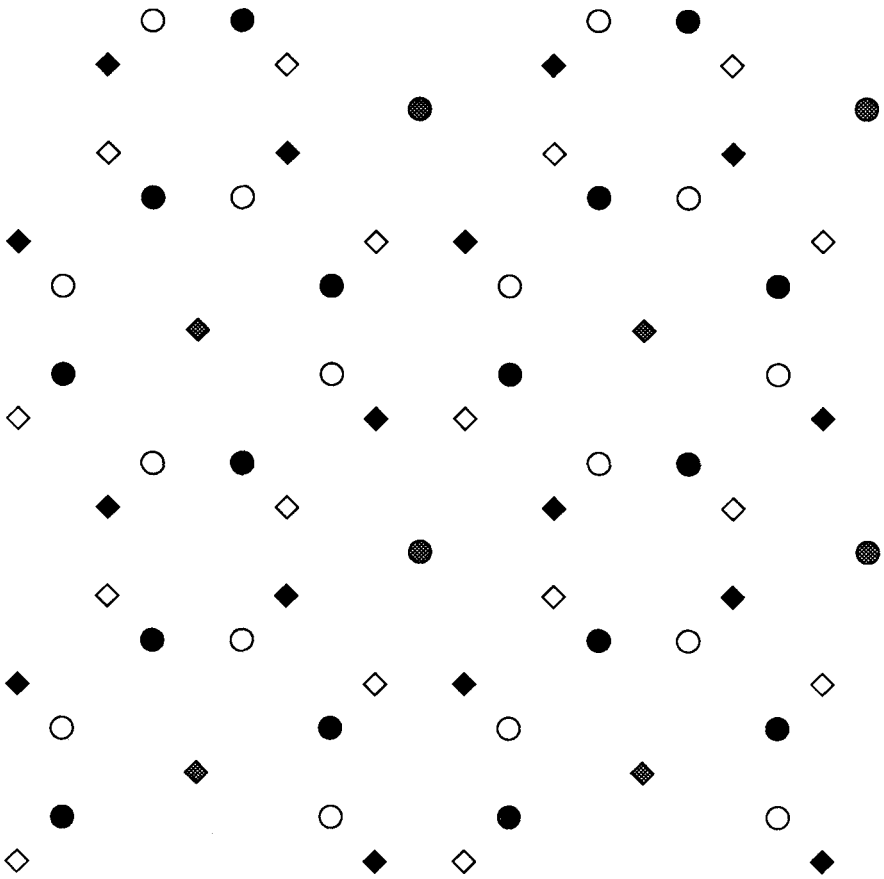

FIG. 6. The unrelaxed type II structure of the Σ5 (001) twist boundary. The symbols have the same meaning as in Fig. 4.

ture is shown in Fig. 5, where the vectors at each atomic site represent the displacements relative to the unrelaxed type I structure. As the temperature was increased, this type I structure remained stable all the way up to the highest temperature investigated, 800 K. An additional series of simulations were performed in which the temperature was decreased (in 100 K increments), starting with the 800 K equilibrium structure (type I). At T = 200 K, the type I structure became unstable and relaxed back into the equilibrium low temperature CSL structure. Finally, a series of simulations were performed at T = 600 K starting from atomic configurations corresponding to the α, β, α', A_1, and type II structures. All of these structures relaxed to the type I structure at this temperature.

The grain boundary Gibbs free energies γ_{gb} for the competing CSL and type I structures are plotted as a function of temperature in Fig. 8. This plot shows that the CSL structure has a lower free energy than the type I structure for all temperatures between 0 K and approximately 315 K. Above 315 K, the type I structure has the lowest free energy. This grain boundary structural transition is clearly first order, since the slope of the free energy changes discontinuously at the transition temperature [see Fig. 8(b) and below]. This is supported by Fig. 9, where the excess volume per unit area of the grain boundary e_{gb} (volume defect or relative rigid shift of the crystals normal to the boundary plane) is plotted as a function of temperature for the CSL and type I structures. e_{gb} undergoes a discontinuous drop at T = 315 K. Finally, we note that the hysteresis observed in determining the grain boundary structure is reminiscent of the hysteresis observed in many other first order phase transitions. However, the detailed form of the hysteresis is undoubtedly influenced by the choice of the simulation procedure.

The excess volume per unit area of grain boundary for the two competing grain boundary structures (Fig. 9) shows that the relaxed CSL structure has a larger volume than the type I structure within the temperature range 300–500 K, where both structures could be observed. However, the thermal expansion of the type I structure (slope of curves in Fig. 9) is clearly greater than that of the CSL structure. At T = 600 K, where the transition from the CSL structure to the type I structure actually takes place in the present simulation, the overall volume of the system decreases by 0.003 Å (times the grain boundary area), and at 200 K where the reverse transition happens, the overall volume of the system increases by 0.006 Å (times the grain boundary area). Since there is a change in volume associated with the grain boundary structural phase transi-

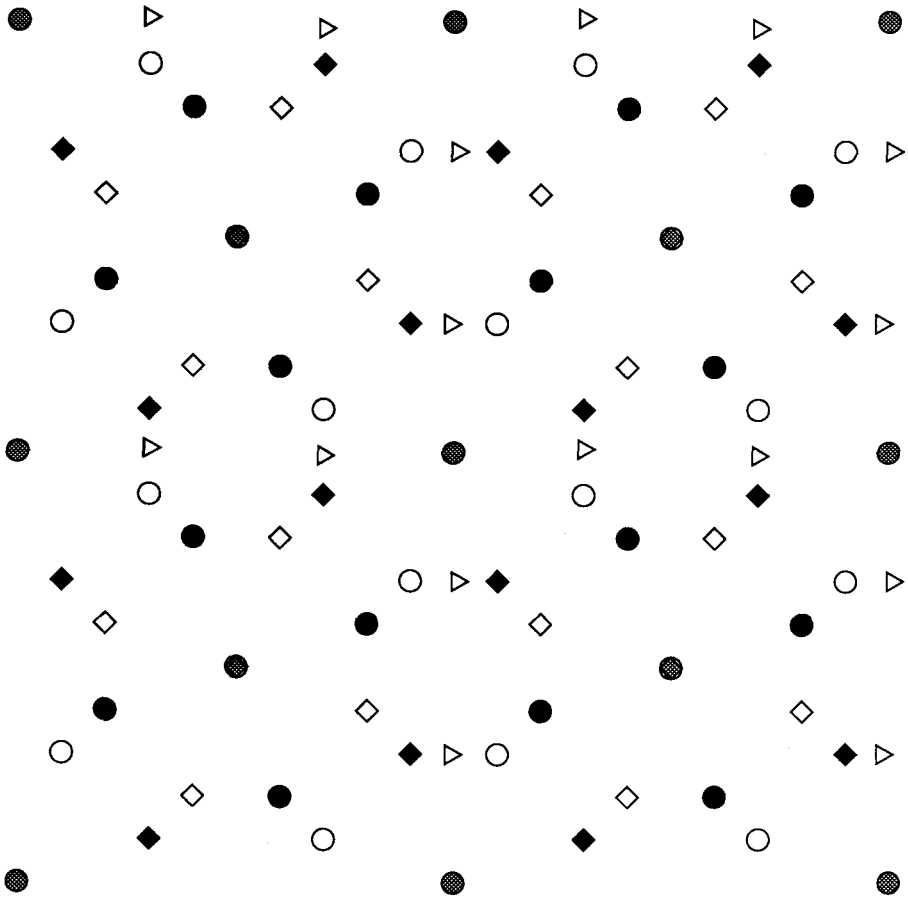

FIG. 7. The unrelaxed $A1$ structure of the Σ5 (001) twist boundary. The symbols have the same meaning as in Fig. 4, except that for this structure an atomic plane (represented by triangles) is coincident with the grain boundary plane.

tion, simulations where the system is kept at fixed volume would hinder the phase transition. Guillope[9] observed a grain boundary structural phase transition in a molecular dynamics study of a tilt boundary in a Lennard–Jones solid. As in the present study, the low temperature structure he observed had a larger excess volume than the high temperature structure.

It is of interest to note that the Σ5 (001) grain boundary expands faster than the perfect crystal (compare Figs. 1 and 9) with increasing temperature (apart

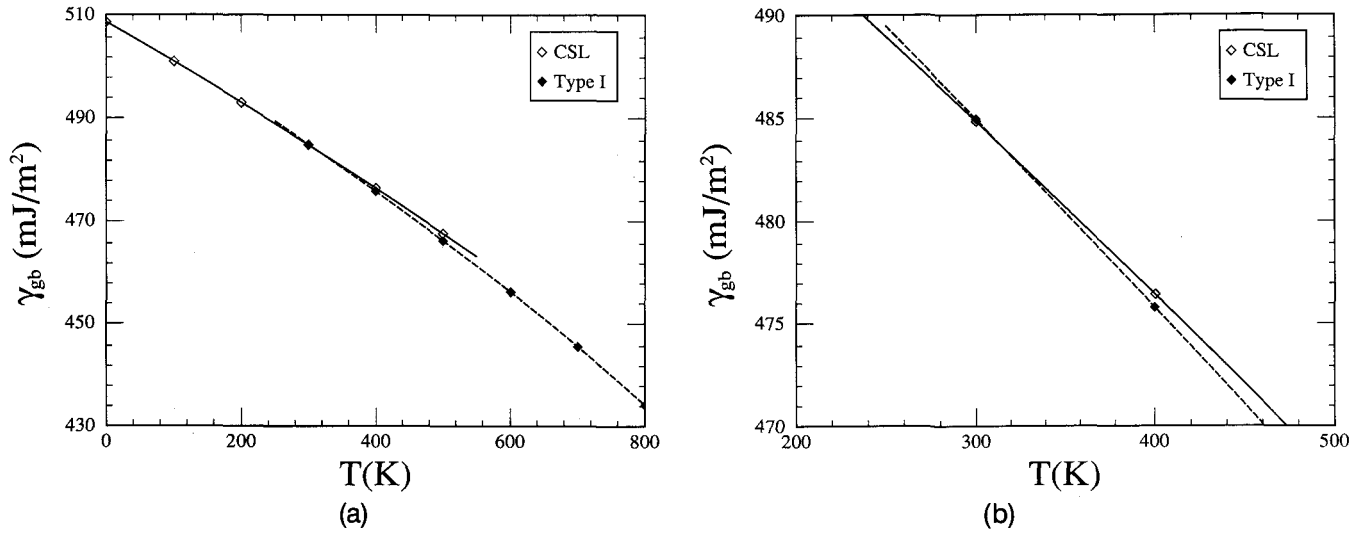

FIG. 8. (a) The grain boundary free energy γ_{gb} versus temperature for the CSL and type I structures. The lines represent polynomial fits to the data points. (b) A close-up of the region where the two lines in (a) cross.

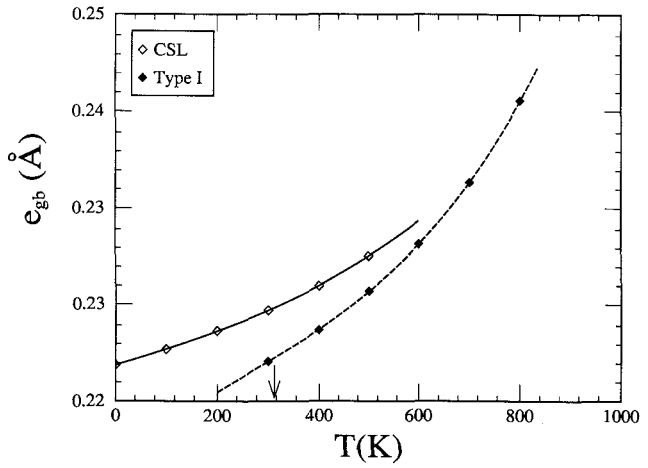

FIG. 9. The excess volume per unit area of grain boundary e_{gb} (or, equivalently, the net expansion associated with the grain boundary) as a function of temperature for the CSL and type I structures. The arrow indicates the transition temperature.

from the discontinuous drop that occurs at the phase transition). This is consistent with recent experiments[22] and simulations[14] on the Σ13 (001) twist boundary in gold. The room temperature value of e_{gb} = 11.1% compares favorably with the experimental value for the Σ5 (001) of 10% ≤ e_{gb} ≤ 18%. The normal strain fields associated with the two competing Σ5 (001) gold twist boundary structures at T = 300 K (CSL: stable, type I: metastable) are shown in Fig. 10 as a function of distance from the boundary plane. In both cases, the majority of the grain boundary expansion occurs at the grain boundary plane itself (between the atomic planes immediately adjacent to the boundary-interplanar spacing n = 0). A net contraction between the first and second layers (n = 1) and a net expansion between the second and third layers are observed. The interplanar spacing between the second and third planes (n = 2) is increased with respect to the perfect crystal interplanar spacing. These expansions and contractions follow exactly the same trend for the CSL and type I structures, although they are slightly smaller for the type I structure. The oscillatory nature of these relaxations is in disagreement with Fitzsimmons and Sass's interpretation of their scattering results,[2] which suggest that the strain decays monotonically away from the grain boundary plane. Nonetheless, we believe that the rapidly damped, oscillatory nature of the strain field on a layer-by-layer basis is real and may be attributed to the dislocation structure of the grain boundaries. The general form of these damped oscillatory strain fields has also been observed in atomistic simulations of tilt boundaries and may be predicted theoretically.[26] The temperature dependent change in the interplanar spacings [$\Delta\epsilon = \epsilon(T) - \epsilon(T = 0)$] between the atomic planes immediately adjacent to the boundary (n = 0) and between the first and second layers (n = 1) is plotted in Fig. 11 for the CSL boundary. This figure demonstrates that the magnitude of the strain associated with the grain boundary decreases with increasing temperature (i.e., the tensile strains become less tensile and the compressive strains become less compressive).

The least ambiguous method for comparing the simulated grain boundary structure with that obtained

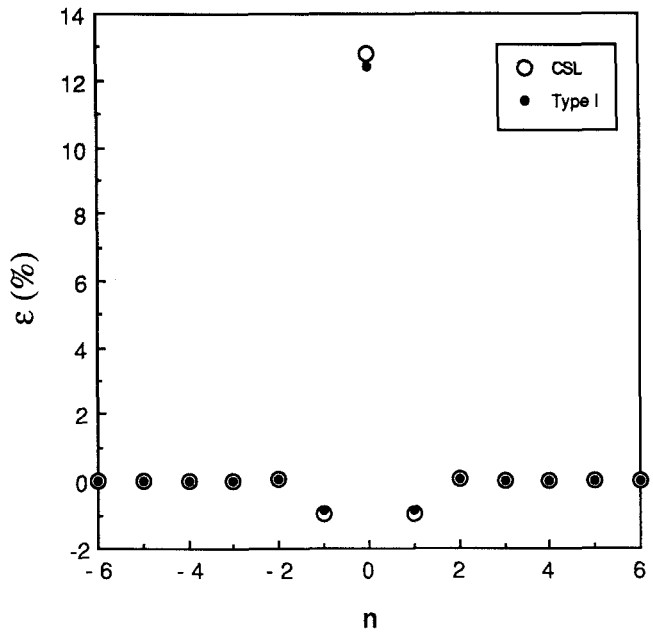

FIG. 10. The strain profile normal to the grain boundary plane ϵ (ϵ_{zz}) for the CSL and type I structures at T = 300 K.

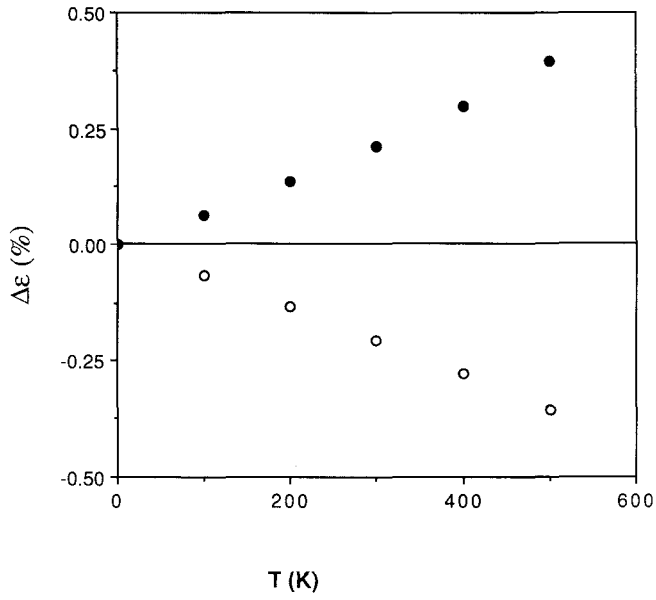

FIG. 11. The change in the strain shown in Fig. 10 as a function of temperature for the CSL structure. The open and solid symbols correspond to the strain at the boundary plane and one (002) interplanar spacing from the boundary. See text for details.

from scattering experiments is via the scattering intensity. For the type I structure this is complicated by the fact that there are two possible equal energy orientations of the type I grain boundary structure. Since these two possible orientations of the type I structure have equal energy, any real type I boundary structure should consist of domains of each orientation. The domain size will be determined by kinetic considerations. On this basis, we assume that the scattering from the type I boundary structure is the linear superposition of the scattering from each of the two possible orientations. Table I shows the scattering intensity for 30 different [H, K] diffraction points (where the scattering amplitude was large or was reported in the literature) corresponding to both the type I and CSL structures at $T = 300$ K and the experimental work of Majid *et al.*[3] and Fitzsimmons and Sass[2] (these data were normalized by the [3, 3] reflection intensity). The experimental scattering intensities were calculated based upon the mean-squared atomic vibrational displacements quoted in each paper,[2,3] while the scattering intensity for the simulated grain boundary structures employed the local vibrational properties of each atom. While the symmetry-averaged type I structure and the CSL structure have the same overall symmetry, the scattering intensity from the two structures shows some marked differences. This is to be expected since the two structures are not equivalent. Likewise, the agreement between the two experimental studies is less than perfect. One particularly striking difference between the experimental and simulation scattering intensities is the absence of scattering from either the CSL or type I structure in the [4, 4] direction and its large intensity in the experimental measurements. Chi-squared measures of the agreement between the simulated structures and the experimental structures were found to be χ^2 (type I—Majid *et al.*) = 0.040, χ^2(CSL—Majid *et al.*) = 0.022, χ^2(type I—Fitzsimmons and Sass) = 0.12, and χ^2(CSL–Fitzsimmons and Sass) = 0.040. Overall, the agreement between our simulations and experiment is better for the CSL structure, which is the equilibrium structure we find at room temperature.

TABLE I. Scattering intensity I_{HKL} for 30 different [$H, K, 0$] diffraction points from the Σ5 (001) twist boundary at $T = 300$ K. The calculated scattering intensities [Eq. (8)] for the two stable grain boundary structures (type I and CSL) and two experimental x-ray determinations[2,3] are listed. The Fitzsimmons and Sass[2] relative intensity data have been scaled to the [3, 3, 0] absolute intensity measured by Majid *et al.*[3]

[H, K]	Type I	CSL	Majid *et al.*[3]	Fitzsimmons and Sass[2]
[1, 0]	0.02	0.00	0.00 ± 0.10	0.00 ± 0.39
[1, 1]	0.02	0.03	0.00 ± 0.19	0.00 ± 0.39
[2, 0]	0.13	0.35	0.96 ± 0.58	0.51 ± 0.32
[2, 1]	0.03	0.14		
[2, 2]	0.01	2.07	2.03 ± 1.01	2.76 ± 0.36
[3, 0]	0.60	0.00	0.00 ± 0.09	0.00 ± 0.30
[3, 2]	0.01	0.23	0.00 ± 0.09	0.17 ± 0.17
[3, 3]	4.83	4.33	5.27 ± 1.84	5.27 ± 0.32
[4, 0]	2.97	3.46	4.01 ± 1.37	6.54 ± 0.38
[4, 1]	0.36	1.10	0.59 ± 0.34	0.27 ± 0.21
[4, 3]	1.93	0.46		
[4, 4]	0.00	0.01	0.95 ± 0.44	2.59 ± 0.31
[5, 0]	0.25	0.00		
[5, 1]	0.24	0.18		0.19 ± 0.14
[5, 2]	0.07	0.30	0.00 ± 0.23	0.00 ± 0.18
[5, 3]	2.98	0.26		0.60 ± 0.26
[5, 4]	0.60	1.93	1.20 ± 0.60	0.78 ± 0.23
[6, 0]	5.77	3.37		
[6, 1]	0.97	1.85	0.90 ± 0.62	0.45 ± 0.37
[6, 3]	0.05	1.17		
[6, 4]	3.88	0.02		0.92 ± 0.31
[6, 5]	0.29	2.98		
[6, 6]	0.55	1.58		
[7, 0]	0.20	0.00	0.00 ± 0.12	0.00 ± 0.14
[7, 2]	1.25	0.58		0.44 ± 0.27
[7, 3]	0.53	0.42		0.31 ± 0.19
[7, 4]	0.93	0.30		
[7, 5]	2.23	3.31		
[7, 6]	0.02	3.04		
[7, 7]	16.81	12.59		

V. THERMODYNAMIC PROPERTIES

All of the thermodynamic properties of a system can be derived from the free energy. Similarly, the excess thermodynamic properties associated with a defect can be derived from the excess free energy of the defect. The temperature dependence of the excess Gibbs free energy per unit area of the Σ5 (001) twist boundary in gold γ_{gb} was presented in Fig. 8 for the type I and CSL structures. The excess entropy per unit area of the grain boundary S_{gb} is derived from Fig. 8 using the identity $S_{gb} = -(\partial\gamma_{gb}/\partial T)_P$. The temperature dependence of S_{gb} is plotted in Fig. 12 for the CSL and type I structures of the Σ5 (001) twist boundary in gold. Both the absolute value and the curvature of the entropy versus temperature curve are larger for the type I structure than for the CSL structure. The larger value of the entropy for the type I structure at all temperatures is consistent with the high temperature stability of that structure. The entropy calculated for Σ5 (001) twist boundary in gold is of the same order of magnitude as that calculated for the Σ13 (001) twist boundary in the same material. Comparison of the excess thermodynamic properties obtained from the simulations with experimental results is difficult due to the problems inherent in making such measurements. Recently, Gleiter and co-workers[27] measured the thermodynamic properties of a nanocrystalline Pd sample from which they attempted to extract the excess grain boundary properties. Using the same assumption for thickness of the grain boundary as used by Gleiter and coworkers, we find $S_{gb}^{experimental} = 5 \times 10^{-3}$ J/(m^2 K),

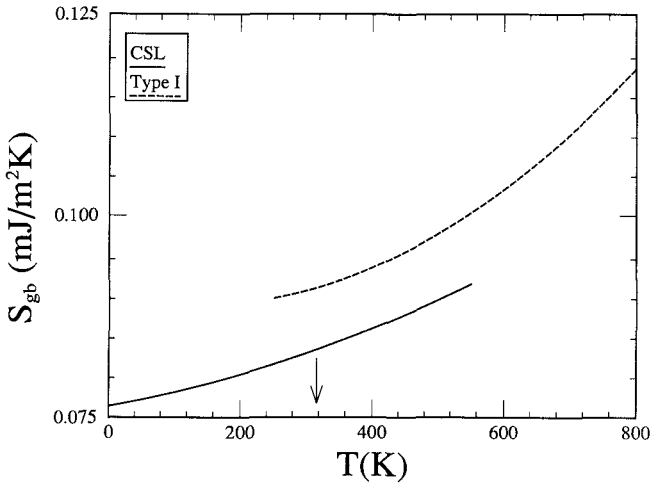

FIG. 12. The excess grain boundary entropy S_{gb} as a function of temperature for the CSL and type I grain boundary structures. These curves were obtained by differentiating the polynomial fit to Fig. 8. The arrow indicates the transition temperature.

which may be compared with the simulation value of 8×10^{-5} J/(m^2 K). This discrepancy far exceeds that which may be expected due to the entropy difference between Au and Pd crystals, which is less than 5%. Possible explanations include (1) the fact that the boundary in the present simulation is higher symmetry (order) than the boundaries in the Pd sample, (2) the presence of defects in addition to grain boundaries in the Pd sample, or (3) the assumption of the number of atoms associated with the grain boundary.

Once the excess free energy and entropy are known, the excess grain boundary enthalpy per unit area H_{gb} may be determined ($H_{gb} = \gamma_{gb} + TS_{gb}$). The temperature dependence of H_{gb} for the Σ5 (001) twist boundary in gold is shown in Fig. 13 for the two competing grain boundary structures. As for the entropy, the magnitude of the enthalpy versus temperature curve is larger for the type I structure than for the CSL structure. The excess specific heat of the grain boundary ($c_p = c_v$ in the present simulation which was performed at $P = 0$) may be determined from the temperature dependence of the enthalpy, $c_{gb} = (\partial H_{gb}/\partial T)_V$. The temperature dependence of the excess grain boundary specific heat per unit area is shown in Fig. 14. At low temperatures the specific heat of the CSL structure exceeds that of the type I structure, while the reverse is true above approximately 350 K. Our 600 K specific heat value exceeds that reported by Sutton[14] for his simulated Σ13 (001) gold twist boundary by approximately a factor of 15. At room temperature, our calculated excess specific heat is less than that reported by Gleiter and co-workers[27] by a factor of roughly 500.

VI. DISCUSSION

Before discussing the simulation results, it is useful to gage their overall reliability. The simulated $T = 0$ relaxed CSL structure is in good agreement with the atomic coordinates reported by Majid *et al.*[3] and the strain profile reported by Wolf and Lutsko[28] obtained using the same gold EAM potential, thereby verifying the accuracy of the procedure employed in the relaxation of the atomic structure. Although neither molecular dynamics nor Monte Carlo thermodynamic data are available on the free energy of this grain boundary using the EAM potential, Monte Carlo data on the free energy of the perfect crystal have recently been published.[20] Since no assumptions regarding the harmonic nature of the atomic vibrations were made in the Monte Carlo calculations, a comparison of the Monte Carlo and LH data provides a test of the LH model. Overall,

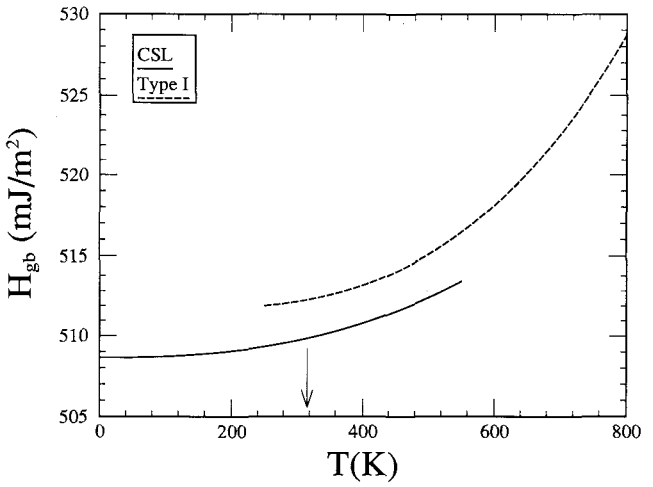

FIG. 13. The excess grain boundary enthalpy H_{gb} as a function of temperature for the CSL and type I grain boundary structures. The arrow indicates the transition temperature.

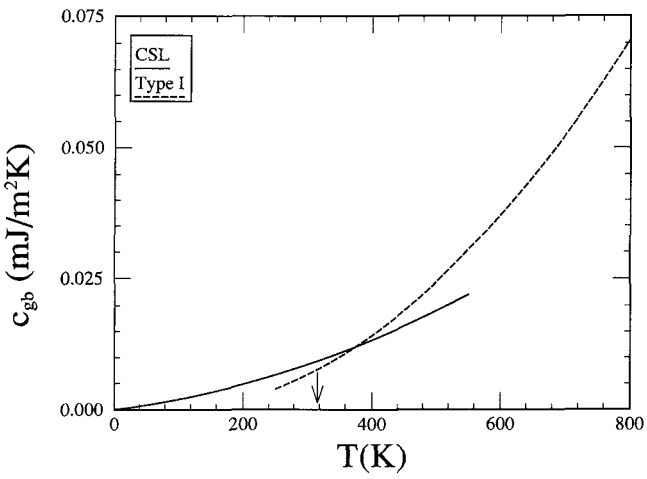

FIG. 14. The excess grain boundary specific heat c_{gb} as a function of temperature for the CSL and type I grain boundary structures. These curves were obtained by differentiating the polynomial fit to Fig. 13. The arrow indicates the transition temperature.

the agreement between the two free energy determinations (see Fig. 1) is excellent, with the LH model consistently predicting a very slightly higher perfect crystal free energy at all temperatures up to three-quarters of the melting point. Agreement among the LH, Monte Carlo, and experimental determinations of the thermodynamic properties of the perfect crystal indicates the high overall accuracy of both the LH model and the EAM potential. Nonetheless, the present simulations are based on an empirical description of the atomic interactions and hence must be viewed with some caution. We do, however, believe that the nature of the general features of the present results transcends the particular choice of the atomic interaction potential (within reason). Since parameters such as the (CSL → type I) transition temperature are very sensitive to small relative changes in the grain boundary free energy, their numerical values may not be very accurate.

Despite all of the recent simulations (including the present one), it is not possible to unequivocally specify the atomic structure of the Σ5 (001) gold twist boundary. Comparison of our room temperature results with the available experimental data suggests that the CSL structure provides a better fit to the experimental data than does the type I structure. This is consistent with the conclusions of Majid *et al.*[3] based upon their $T = 0$ calculation. The difficulty in obtaining agreement between simulation and experiment for this grain boundary may be attributable to the presence of a grain boundary phase transition very near the temperature at which the experiment was performed. The proximity of the temperature at which the experimental measurements were made to the phase transition temperature can have two distinct effects. First, critical phenomena associated with the transition may play an as-yet-unaccounted-for role in the scattering. Second, since the experimental samples were prepared at temperatures in excess of the transition temperature and cooled to just slightly below it, the driving force (undercooling) for the transformation may be insufficient to drive the transformation to completion. This could lead to a grain boundary structure which is a metastable mix of the two high temperature, type I structures and the CSL structure or possibly to another type of metastable structure. Such a mixed phase structure may lead to better agreement with experiment. However, since it would be metastable, the mixed structure cannot be determined without careful consideration of the transformation kinetics.

The present report represents one of the few systematic simulation studies of the thermodynamic properties of grain boundaries over a wide temperature range. As a consequence, there are relatively few other data to compare with, and hence the generality of the present results remains unknown. However, our unpublished results on other gold twist boundaries confirm the general thermodynamic features observed in the present simulation, including the presence of first order phase transitions. Comparison with experimental data presents even a greater problem, since no direct experimental measure of the excess thermodynamic properties of grain boundaries is available. The disagreement between our results and the nanocrystalline Pd results is probably due to the difficulty of interpreting the experimental results.

The (CSL → type I) grain boundary phase transformation observed in the present simulations is unquestionably first order. Two types of second order grain boundary phase transitions have been investigated previously: one associated with structural disordering[10] and the other with the vanishing of cusps in the interfacial variables.[29] Rottman[17] suggests that first order grain boundary phase transitions may be quite common. This is consistent with our observations that a substantial fraction of the grain boundaries which we have studied to date undergoes first order phase transitions. It is our hope that this paper will lead to more experimental studies of the structure and properties of grain boundaries as a function of temperature.

VII. CONCLUSION

We have performed a systematic simulation study of the thermodynamic properties of the Σ5 (001) (36.9°) twist boundary as a function of temperature. This study was performed within the framework of the Local Harmonic (LH) model and employed an Embedded Atom Method (EAM) potential for gold. We find that for the Σ5 (001) twist boundary in gold, a distorted CSL structure is stable at low temperatures, but undergoes a phase transformation to a DSC related structure near room temperature. This transformation is shown to be first order. The temperature dependences of the excess grain boundary free energy, enthalpy, entropy, and specific heat are calculated. Discontinuities are observed in the slope of the grain boundary excess free energy (versus temperature), in the value of the grain boundary excess specific heat and excess volume. The stable high temperature grain boundary structure has a smaller excess volume than does the lower temperature structure, and both structures have a coefficient of thermal expansion which is in excess of that for the perfect crystal.

ACKNOWLEDGMENTS

We thank Adrian Sutton for bringing the similarities between his simulation method and the LH model to our attention. We gratefully acknowledge the support of the Office of Basic Energy Sciences of the United States Department of Energy (R. N. and D. J. S's

work was performed under Grant No. FG02-88ER-45367), under whose auspices the present research was conducted. R. L. would like to thank the Departments of Chemistry and Materials Science and Engineering of the University of Michigan for their hospitality during his stay.

REFERENCES

[1]J. Budai, P. D. Bristowe, and S. L. Sass, Acta Metall. **31**, 699 (1983).
[2]M. R. Fitzsimmons and S. L. Sass, Acta Metall. **36**, 3103 (1988).
[3]I. Majid, P. D. Bristowe, and R.W. Balluffi, Phys. Rev. B **40**, 2779 (1989).
[4]M. R. Fitzsimmons and S. L. Sass, Acta Metall. **36**, 1009 (1988).
[5]P. D. Bristowe and S. L. Sass, Acta Metall. **28**, 575 (1980).
[6]R. Najafabadi, D. J. Srolovitz, and R. A. LeSar, Scripta Metall. **24**, 251 (1990).
[7]M. R. Fitzsimmons, M. D. Vaudin, and S. L. Sass, Scripta Metall. **22**, 105 (1988).
[8]R.W. Balluffi and T. E. Hsieh, J. Phys. (Paris) **49**, C5-337 (1988).
[9]M. Guillope, J. Phys. (Paris) **47**, 1347 (1986).
[10]V. Vitek, Y. Minonishi, and G. J. Wang, J. Phys. (Paris) **46**, C4-243 (1985).
[11]F. Carrion, G. Kalonji, and S. Yip, Scripta Metall. **17**, 915 (1983).
[12]P. Deymier, A. Taiwo, and G. Kalonji, Acta Metall. **35**, 2719 (1987).
[13]P. Deymier and G. Kalonji, J. Phys. (Paris) **46**, C4-213 (1985).
[14]A. P. Sutton, Philos. Mag. A **60**, 147 (1989).
[15]L. Q. Chen and G. Kalonji, Philos. Mag. A **60**, 525 (1989).
[16]J. F. Lutsko, D. Wolf, and S. Yip, J. Phys. (Paris) **49**, C5-375 (1988).
[17]C. Rottman, J. Phys. (Paris) **49**, C5-313 (1988).
[18]R. LeSar, R. Najafabadi, and D. J. Srolovitz, Phys. Rev. Lett. **63**, 624 (1989).
[19]S. M. Foiles, M. I. Baskes, and M. S. Daw, Phys. Rev. B **33**, 7983 (1986).
[20]S. M. Foiles and G. B. Adams, Phys. Rev. B **40**, 5909 (1989).
[21]R. Hultgren, P. D. Desai, D. T. Hawkins, M. Gleiser, K. K. Kelley, and D. D. Wagman, *Selected Values of the Thermodynamic Properties of the Elements* (ASM, Metals Park, OH, 1973).
[22]M. R. Fitzsimmons, E. Burkel, and S. L. Sass, Phys. Rev. Lett. **61**, 2237 (1988).
[23]P. D. Bristowe and A. G. Crocker, Philos. Mag. A **38**, 487 (1978).
[24]W. Bollman, *Crystal Defects and Crystalline Interfaces* (Springer, Berlin, 1970).
[25]Y. Oh and V. Vitek, Acta Metall. **34**, 1941 (1986).
[26]S. P. Chen, A. F. Voter, and D. J. Srolovitz, J. Mater. Res. **4**, 64 (1989).
[27]D. Korn, A. Morsch, R. Birringer, W. Arnold, and H. Gleiter, J. Phys. (Paris) **49**, C5-769 (1988).
[28]D. Wolf and J. F. Lutsko, J. Mater. Res. **4**, 1427 (1989).
[29]H. Kuhn, G. Baero, and H. Gleiter, Acta Metall. **27**, 959 (1979).